Parametric Controller Design and Optimization for A Brushless DC Motor System

Jinbo Lu Xiaorong Hou Min Luo
School of Energy Science and Engineering
University of Electronic Science and Technology of China
No.2006, Xiyuan Ave, West Hi-Tech Zone, Chengdu, Sichuan, P.R.China
houxr@uestc.edu.cn

Abstract: - In this paper, a research on the design of parametric controller has been presented for a brushless DC motor system, and the parameters of controller are optimized. Compared with PID, the overshoot of state curve is smaller, and the settling time is shorter. The symbolic computation and the cylindrical algebraic decomposition (CAD) are used in controller design and controller parameters calculation. Symbolic computation is applied to obtain the stable constraints for the controlled system. And the region of controller parameters can be solved by CAD, according to the constraints. The parameters of controller selected in the region will stabilize the brushless DC motor system. And then, the system dynamic performance can be optimized by a variable parameter control of designed controller. The simulation results indicate that the proposed method is highly effective in controlling the brushless DC motor system.

Key-Words: - Symbolic computation, parametric controller, Hopf bifurcation, cylindrical algebraic decomposition (CAD), brushless DC motor, optimization.

1 Introduction

With the development of permanent magnetic materials and control technology, brushless DC motor has been widely applied because of its power density, simple structure, easy control, robustness, and convenient maintenance [1, 2]. Therefore, the brushless DC motor control technology has a significant theoretical and practical importance. In recent years, a large number of researchers have studied the brushless DC motor system control [3, 4, 14]. Samitha et al. [3] presents a torque ripple compensation technique for a brushless DC motor torque control that is operated without a DC link capacitor. Nian et al. [4] studied the regenerative braking system of brushless DC motor, using PID control.

The parametric control system has shown many advantages, and has been applied to a wide range in engineering [11-13, 15-18]. However, there are only a few studies on the application of parametric controller to brushless DC motor control system. In this paper, a parametric controller is designed by symbolic computation and cylindrical algebraic decomposition.

The symbolic computation, also known as computer algebra, is a powerful approach in solving the tough and intricate problems in applied mathematics. In the last two decades, symbolic computation has made a significant impact in many fields of science and engineering [5-7, 10]. The symbolic method can be effectively used to handle the nonlinear optimization. In fact, symbolic computation and its methods have been extensively used in nonlinear system control. Since a lot of analysis and design problems of the multi-agent dynamic systems are reduced to nonlinear feasibility or optimization problems, symbolic computation may effectively work to derive the exact solutions. Hara et al. [5] used the symbolic computation in analysis and synthesis for multi-agent dynamical systems, where all the agents share a common Linear Time Invariant (LTI) system. Zhang et al. [6] discussed the symbolic computation of normal form for Hopf bifurcation in a neutral delay differential equation. In [7], Freitas et al. applying symbolic computation and numerical calculations, describes a symbolic–numerical integration method for a class of differential algebraic equations (DAEs) known as semi-explicit systems.

The constraints of the parametric controller can be obtained using the symbolic computation. These constraints are usually composed of inequalities, and it is difficult to solve for the parameters from the inequalities. There are very few methods that can be applied to this problem, including CAD. In this paper, the CAD method [8, 9] is used to convert inequalities into the segmentation of parameters space.

In design of control system, when the range of available controller parameters is large, the

performance of the control system more easy to achieve and optimize. The proposed method uses symbolic computation and CAD to completely solve the controller parameters, and obtain more large range of available parameters in comparison to the existing studies [3, 14]. And the simulations show that the designed controller is much better than PID. Then, the rest of this paper is organized as follows. The brushless DC motor system and the parametric controller design method are presented in Section II. In Sections III, symbolic computation is applied to obtain the stable constraints of the controller. In Section IV, the method to obtain the stable region of controller parameters is explained. Simulations and parameters optimization are discussed in Section V. And the conclusions are given in Section VI.

2 The Brushless DC System Description and Parametric Controller Design

Before discussing the parametric controller, the brushless DC motor system [19] is described as:

$$\begin{cases} \dot{x} = -x - yz + 17z + v_q \\ \dot{y} = -y + xz \\ \dot{z} = 4(x - z) - T_L \end{cases} \tag{1}$$

where, x, y and z are the states of the system, v_q is equivalent driving potential, and T_L is the equivalent load of the motor. In the system (1) $v_q = 1$, and $T_L \in [0, 0.2]$. T_L is uncertainty and it is considered as a disturbance here. T_L is defined as a sin function of time in the simulations, and it is taken as $T_L = 0$ for the calculation of controller parameters. The equilibrium of system (1) is $E_0 = (x_0, y_0, z_0)$, which can be solved out from the follows:

$$y_0 = x_0 z_0 \tag{2}$$

$$x_0 = z_0 \tag{3}$$

$$G(z_0) = -z_0^3 + 16z_0 + 1 = 0 \tag{4}$$

so

$$z_{01} \approx -3.9684,\ z_{02} \approx -0.062515,\ z_{03} \approx 4.0309 \tag{5}$$

Then the equilibria of the system (1) are:

$$E_{01} = (-3.9684, 15.748, -3.9684),$$

$$E_{02} = (-0.062515, 0.003908, -0.062515),$$

$$E_{03} = (4.0309, 16.248, 4.0309).$$

The system trajectory is chaotic at equilibrium in the system (1) without controller.

Theorem 1: For system (1), the controller is designed as:

$$u(x, y, z) = g(x, y, z)\dot{x} + c_{01}\dot{y} + c_{02}\dot{z} \tag{6}$$

where, $g(x, y, z) = c_1 + c_2 x + c_3 y + c_4 z$, $\{c_i \in R, i = 1, 2, 3, 4\}$, $c_{01} \in R$, $c_{02} \in R$. The controlled blushless DC motor system can be written as:

$$\begin{cases} \dot{x} = -x - yz + 17z + 1 + u(x, y, z) \\ \dot{y} = -y + xz \\ \dot{z} = 4(x - z) - T_L \end{cases} \tag{7}$$

Then choose the appropriate values of c_1, c_2, c_3, c_4, c_{01} and c_{02} the system (7) will be controlled.

Proof:

In order to simplify the calculation, the coefficients values of $c_{01} = c_0$ and $c_{02} = 0$ are considered. Using symbolic computation, the Jacobian of system (7) at equilibrium is given as:

$$J = \begin{bmatrix} j_{11} & j_{12} & j_{13} \\ z_0 & -1 & z_0 \\ 4 & 0 & -4 \end{bmatrix} \tag{8}$$

where,

$$j_{11} = -c_2 z_0^3 - c_3 z_0^2 + 15c_2 z_0 - c_4 z_0 + 4c_0 - c_1 + c_2 - 1 \tag{9}$$

$$j_{12} = -2c_3 z_0^3 - (c_2 + c_4) z_0^2 - (c_1 - 16c_3 + 1) z_0 + c_3 \tag{10}$$

$$j_{12} = -c_3 z_0^4 - (c_2 + 2c_4) z_0^3 - (c_1 - 17c_3 + 1) z_0^2 + (17c_2 + 33c_4) z_0 - 4c_0 + 17c_1 + c_4 + 17 \tag{11}$$

According to (2), (3), and (8), the system characteristic equation at the equilibrium is derived as:

$$D(\lambda) = a_0 \lambda^3 + a_1 \lambda^2 + a_2 \lambda + a_3 \tag{12}$$

where,

$$a_0 = 1 \tag{13}$$

$$a_1 = c_3 z_0^2 + c_4 z_0 + c_2 z_0 - 4c_0 + 6 + c_1 \tag{14}$$

$$a_2 = 5c_1 z_0^2 + 17c_3 z_0^2 + 5z_0^2 + 17c_2 z_0 + 5c_3 z_0 + 17c_4 z_0 - 4c_0 - 63c_1 + 5c_2 + 5c_4 - 59 \tag{15}$$

$$a_3 = 12c_1 z_0^2 + 128c_3 z_0^2 + 12z_0^2 + 128c_2 z_0 + 12c_3 z_0 + 128c_4 z_0 - 64c_1 + 12c_2 + 12c_4 - 64 \tag{16}$$

In order to control the system at equilibrium, from the Hurwitz criterion, the system parameters need to satisfy the following conditions.

$$\begin{cases} a_i > 0, \quad i = 0, 1, 2, 3 \\ g = a_1 a_2 - a_0 a_3 \geq 0 \end{cases} \tag{17}$$

Then choose the appropriate values of parameters c_0, c_1, c_2, c_3 and c_4 to satisfy conditions (17), and the system (7) will be controlled.

Remark1: In order to simplify the calculation, the coefficients of system characteristic equation (12) are divided by the polynomial $-z_0^3+16z_0+1$ of equilibrium equation (4), whose value is zero at equilibrium, and (14) - (16) are the remainders.

Remark2: The inequities in (17) are the system stability constraints. Here $a_i>0$ must be satisfied, if there is no static bifurcation in system. $g>0$ is a stability condition and $g=0$ is the supercritical Hopf bifurcation condition. Since the motor control is a real problem, only the stable state is considered in this paper. Practically, the formula (17) is composed of many inequalities. It is very difficult to completely solve these inequalities. In this paper the problem of solving inequalities can be transformed into a number of parameter space partition problems in a multidimensional space.

3 Constraints Computation

To be more simplify, $c_2=0$, $c_4=0$ are chosen. Based on the equation (5), the system stable constraints at z_{01}, z_{02}, z_{03} can be written as following.

At $z_{01}\approx -3.9684$,

$$a_{101}=-4c_0+c_1+15.748c_3+6 \tag{18}$$

$$a_{201}=-4c_0+15.741c_1+247.88c_3+19.741 \tag{19}$$

$$a_{301}=124.98c_1+1968.15c_3+124.98 \tag{20}$$

$$\begin{aligned}g_{01}=&16c_0^2+15.741c_1^2+3903.6c_3^2-66.964c_0c_1\\&-1054.5c_0c_3+495.75c_1c_3-102.96c_0\\&-10.791c_1-170.01c_3-6.5324\end{aligned} \tag{21}$$

At $z_{02}\approx -0.062515$,

$$a_{102}=-4c_0+c_1+0.0039081c_3+6 \tag{22}$$

$$a_{202}=-4c_0-62.98c_1-0.24614c_3-58.98 \tag{23}$$

$$a_{302}=-63.953c_1-0.24994c_3-63.953 \tag{24}$$

$$\begin{aligned}g_{02}=&16c_0^2-62.98c_1^2-0.00094494c_3^2\\&+247.92c_0c_1+0.96891c_0c_3\\&-0.49227c_1c_3+211.92c_0-372.91c_1\\&-1.4574c_3-289.93\end{aligned} \tag{25}$$

At $z_{03}\approx 4.0309$

$$a_{103}=-4c_0+c_1+16.248c_3+6 \tag{26}$$

$$a_{203}=-4c_0+18.241c_1+296.37c_3+22.241 \tag{27}$$

$$a_{303}=130.98c_1+2128.13c_3+130.98 \tag{28}$$

$$\begin{aligned}g_{03}=&16c_0^2+18.241c_1^2+4815.5c_3^2-76.963c_0c_1\\&-1250.5c_0c_3+592.75c_1c_3-112.96c_0\\&+0.70756c_1+11.47c_3+2.4668\end{aligned} \tag{29}$$

From a_{301}, a_{302}, a_{303}, following can be obtained:

$$\begin{cases}-1-15.748c_3<c_1\\c_1<-1-0.0039082c_3\\-1-16.248c_3<c_1\end{cases} \tag{30}$$

when $c_3\le 0$ in the inequities (30), c_1 does not exist to satisfy the inequalities. So $c_3>0$, and $c_3=1$ is selected. The equations (18)-(29) can be rewritten as:

$$a_{101}=-4c_0+c_1+21.748 \tag{31}$$

$$a_{201}=-4c_0+15.741c_1+267.62 \tag{32}$$

$$a_{301}=124.98c_1+2093.1\approx 124.98(c_1+16.748) \tag{33}$$

$$\begin{aligned}g_{01}=&16c_0^2+15.741c_1^2-66.964c_0c_1-1157.5c_0\\&+484.96c_1+3727\end{aligned} \tag{34}$$

$$a_{102}=-4c_0+c_1+6.0039 \tag{35}$$

$$a_{202}=-4c_0-62.98c_1-59.227 \tag{36}$$

$$\begin{aligned}a_{302}=&-63.953c_1-64.203\\\approx&-63.953(c_1+1.0039)\end{aligned} \tag{37}$$

$$\begin{aligned}g_{02}=&16c_0^2-62.98c_1^2+247.92c_0c_1+212.89c_0\\&-373.4c_1-291.39\end{aligned} \tag{38}$$

$$a_{103}=-4c_0+c_1+22.248 \tag{39}$$

$$a_{203}=-4c_0+18.241c_1+318.61 \tag{40}$$

$$\begin{aligned}a_{303}=&130.98c_1+2259.1\\\approx&130.98(c_1+17.248)\end{aligned} \tag{41}$$

$$\begin{aligned}g_{03}=&16c_0^2+18.241c_1^2-76.963c_0c_1-1363.4c_0\\&+593.45c_1+4829.4\end{aligned} \tag{42}$$

4 Using CAD to Solve the Range of Controller Parameters

The stability constraints of the system (7) are composed of the equations (31)-(42), and the curves of equalities (31) to (42) have been drawn on c_0-c_1 plane. The plane is divided into 63 regions, as shown in Fig. 1. The parameters c_0 and c_1 in each region are tested to find the one in which the values can satisfy the stability constraints. Finally, region 30 is obtained, where the parameters c_0 and c_1 of controller can provide a stable control of the brushless DC

motor system. Region 30 is contained with the lines $a_{301}=0$, $a_{302}=0$, and $g_{02}=0$.

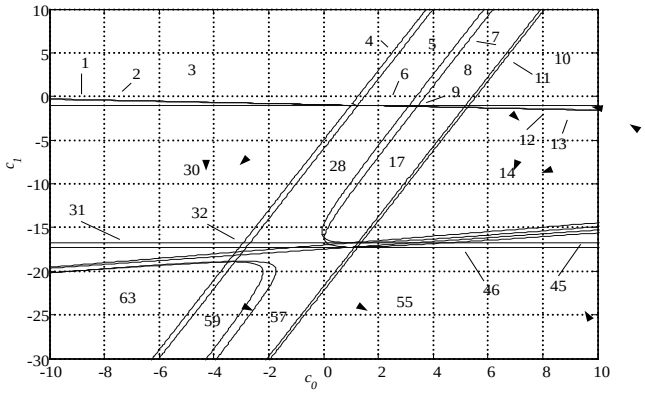

Fig. 1 The partition of the system stability constraints in the c_0-c_1 plane

5 Simulations and Parameters Optimization

Through the above calculation, the range in which the controller parameters can satisfy the stability requirements is obtained. The trajectory of system (1) is chaotic without the controller (see Fig. 2).

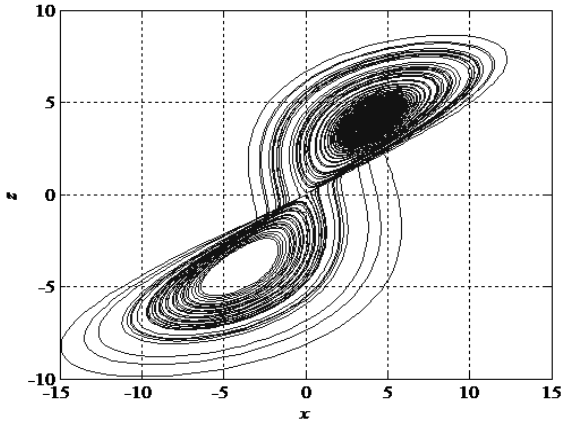

Fig. 2 The system trajectory without control

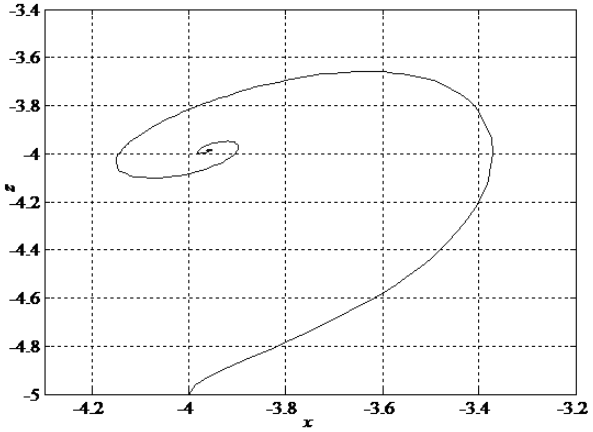

Fig. 3 The system trajectory at E_{01}

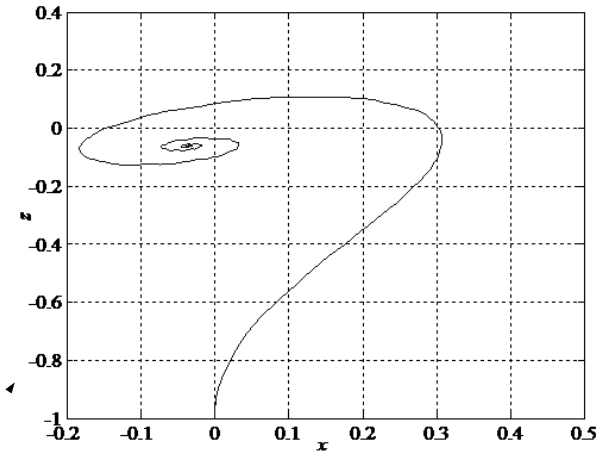

Fig. 4 the system trajectory at E_{02}

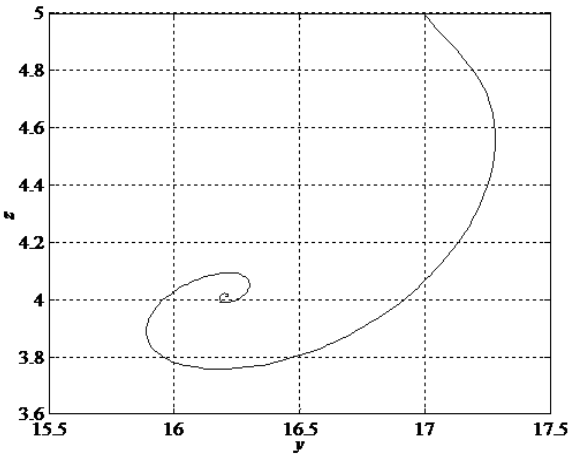

Fig. 5 the system trajectory at E_{03}

The controller parameters $\{c_0=0, c_1=-2\}$ are chosen to verify the effectiveness of parameters. The initial values of the states for system (1) are $(-4,17,-5)$ (for E_{01}), $(0,1,-1)$ (for E_{02}), $(4,17,5)$ (For E_{03}). $T_L=0.1\sin(20\pi t)+0.1$ is chosen for the verification. The system trajectories at equilibria are shown in Fig. 3 to Fig. 5. It can be seen from the figures that the trajectories of the controlled system are convergent, resulting in a stable system.

In order to further illustrate the benefits of using CAD to solve the controller parameters, the controller parameters are optimized. The variable parameter control is tried at equilibrium E_{02}. The control parameters are switched between $\{c_0=0, c_1=-2\}$ and $\{c_0=-5, c_1=-10\}$ during different time periods. The switching condition is given as:

$$\begin{cases} c_0 = 0, c_1 = -2 & while \quad 0 \le t < 0.148 \\ c_0 = -5, c_1 = -10 & while \quad 0.148 \le t \le 0.78 \\ c_0 = 0, c_1 = -2 & while \quad 0.78 < t \le 5 \end{cases} \quad (43)$$

It is easy to see from Fig.6 that curve 1 and curve 3 intersect at $t = 0.148$ and $t = 0.78$. When $0 \le t < 0.148$, we select $\{c_0 = 0, c_1 = -2\}$ to reduce the overshoot, and select $\{c_0 = -5, c_1 = -10\}$ when $0.148 \le t \le 0.78$, select $\{c_0 = 0, c_1 = -2\}$ when $0.78 < t \le 5$ to shorten settling time.

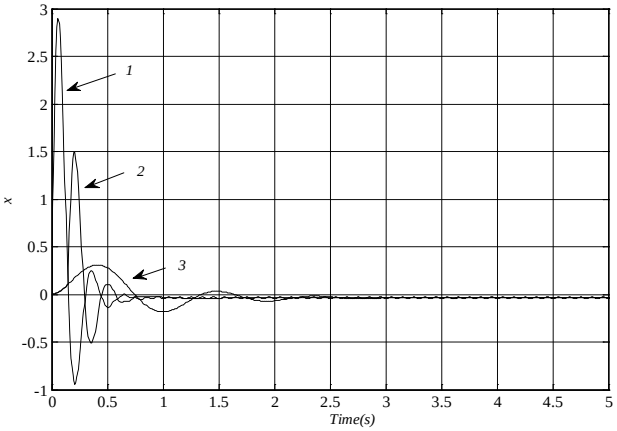

Fig. 6 State x adjustment curves under different parameters

The initial value of system states at E_{02} is $(0,1,-1)$. The simulation of state x is shown in Fig. 6. There are three curves in the figure. Curve 2 is the state x curve with the variable parameter control in equation (43). Curve 1 is the response of state x when $\{c_0 = 0, c_1 = -2\}$ and Curve 3 is the response when $\{c_0 = -5, c_1 = -10\}$. The overshoot of curve 1 is maximum ($x = 2.9$, at $t = 0.058s$) and settling time is shortest ($t = 0.7s$). Curve 3 has the minimum overshoot ($x = 0.31$, at $t = 0.47s$) and the longest settling time ($t = 1.73s$). Due to the use of variable parameter control, the overshoot of curve 2 is smaller ($x = 1.5$, at $t = 0.2s$) and settling time is shorter ($t = 0.78s$). Compared to the curve 1, the overshoot is reduced by 48% and settling time is increased by only 11%. Similarly in comparison to the curve 3, the settling time is reduced by 55%. The figure illustrates that the state performance of the system is optimized, when the controller parameters c_0 and c_1 vary according to the equation (43). The curve of state x under the PID control is shown in Fig. 7. And it is can be seen that both overshoot and settling time of the designed controller in Fig. 6 are obviously much better than that of PID in Fig. 7.

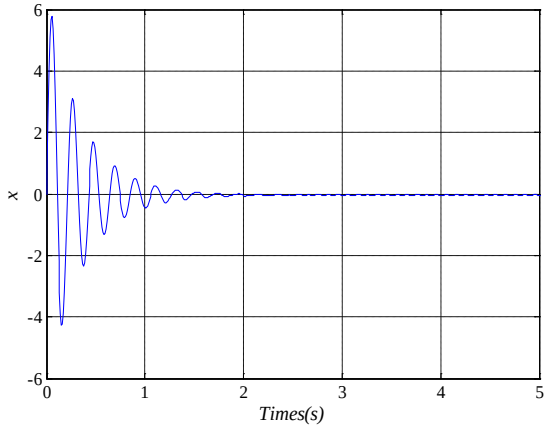

Fig. 7 State x curve under PID control

The simulation results in the Fig. 3 to Fig. 6 show that the symbolic computation and CAD in parametric controller design can be successfully applied to a practical system, and the control performance optimization is feasible by changing the controller parameters in the stable range (Region 30 in Fig. 1).

6 Conclusion

The symbolic computation and CAD are applied to a parametric controller design for a brushless DC motor. The range of parameters to control the system is obtained. The simulation results show that the system can be stabilized at equilibrium with the proposed controller, even in the presence of a disturbance (as $T_L = 0.1\sin(20\pi t) + 0.1$), and the effects of the controller are much better than PID. To further study the impact of control parameters on the system performance, the parameter optimization is discussed. The numerical results illustrate the effectiveness of the optimization.

References:

[1] M. Oshima, C. Takeuchi, Magnetic Suspension Performance of a Bearingless Brushless DC Motor for Small Liquid Pumps, *IEEE Transactions on Industry Applications*, Vol.47, Iss.1, 2010, pp. 72–78.

[2] V. Bist, B. Singh, A Brushless DC Motor Drive With Power Factor Correction Using Isolated

Zeta Converter, *IEEE Transactions on Industrial Informatics*, Vol.10, Iss.4, 2014, pp. 2064 - 2072.

[3] H. Samitha, U. Madawala, A Torque Ripple Compensation Technique for a Low-Cost Brushless DC Motor Drive, *IEEE Transactions on Industrial Electronics*, Vol.62, Iss.10, 2015, pp. 6171 - 6182.

[4] X. Nian, Regenerative Braking System of Electric Vehicle Driven by Brushless DC Motor, *IEEE Transactions on Industrial Electronics*, Vol.61, Iss.10, 2014, pp. 5798 - 5808.

[5] S. Hara and H. Anai, Symbolic Computation in Analysis and Synthesis for Homogeneous Multi-agent Dynamical Systems, *IEEE Conference on International Symposium on Computer-Aided Control System Design*, Yokohama, Japan, 2010, pp. 1702-1707.

[6] L. Zhang, H. Wang, H. Hu, Symbolic Computation of Normal Form for Hopf Bifurcation in A Neutral Delay Differential Equation and An Application to A Controlled Crane, *Nonlinear Dynamics*, Vol.70, Iss.1, 2012, pp. 463-473.

[7] C. Freitas, P. Silva, A Symbolic–Numerical Method for Integration of DAEs Based on Geometric Control Theory, *Journal of Control, Automation and Electrical Systems*, Vol.25, Iss.4, 2014, pp. 400-412.

[8] H. Hjalmarsson and F. Egebrand, Input design using cylindrical algebraic decomposition, *The 50th IEEE Conference on Decision and Control and European Control Conference (CDC-ECC)*, Orlando, USA, 2011, pp.811-817.

[9] I. Fotiou, P. Parrilo and M. Morari, Nonlinear parametric optimization using cylindrical algebraic decomposition, *The 44th IEEE Conference on Decision and Control, and the European Control Conference*, Seville, Spain, 2005, pp. 3735-3740.

[10] T. Lee, A contemporary engineering perspective on symbolic computation, *ICROS-SICE International Joint Conference*, Fukuoka, Japan, 2009, pp. 2379-2384.

[11] D. Wong and B. Hencey, A Controller Switching Design Approach via Parameterization for Control of Hard Disk Drive Dual-Stage Actuators, *American Control Conference (ACC)*, Washington, DC, USA, 2013, pp. 836-841.

[12] K. Mori, Controller Parameterization of Anantharam's Example, *IEEE Transactions on Automatic Control*, vol. 48, no. 9, 2003, pp.1655-1656.

[13] V. Kamenetskii, Parametric Stabilization of Automatic Control Systems, *Automation and Remote Control*, Vol.72, Iss.11, 2011, pp. 2300-2314.

[14] M. Zhou, Z. Li, Q. Gu, and Z. Xu, Influence of PWM Modes on Non-Commutation Torque Ripple in Brushless DC Motor Control System, *The 2nd International Conference on Measurement, Information and Control*, China, 2013, pp. 1004-1008.

[15] Y. Choi and W. Chung, On the Stable $H\infty$ Controller Parameterization Under Sufficient Condition, *IEEE Transactions on Automatic Control*, vol. 46, no. 10, pp. 1618-1623, 2001.

[16] T. Sakanushi, K. Yamada and J. Hu, The Parameterization of All Robust Stabilizing Simple Multi-Period Repetitive Controllers for Multiple-Input/Multiple-Output Plants with Specified Input-Output Frequency Characteristic, *American Control Conference (ACC)*, Washington, DC, USA, 2013, pp 1870-1875.

[17] A. Anisimov, D. Kotov, S. Tararykin, et al, Analysis of Parametric Sensitivity and Structural Optimization of Modal Control Systems with State Controllers, *Journal of Computer and Systems Sciences International*, Vol.50, Iss.5, 2011, pp. 698-713.

[18] M. Ruderman, Tracking Control of Motor Drives Using Feedforward Friction Observer, *IEEE Transactions on Industrial Electronics*, Vol.61, Iss.7, 2013, pp. 3727 - 3735.

[19] Z. Zhang，H. Yuan，Y. Zhang, Bifurcation Analysis and Hopf Bifurcation Control of a Motor System, *Acta Armamentarii*, vol. 34, no. 8, 2013, pp. 1051-1056.